

# Simultaneous FTIR/UV-Vis study of reactions over metallo-zeolites Approach to quantitative *in situ* studies

Zdenek Sobalík<sup>a,\*</sup>, Kamil Jíša<sup>a</sup>, Hana Jirglová<sup>a</sup>, Bohumil Bernauer<sup>b</sup>

<sup>a</sup> J. Heyrovský Institute of Physical Chemistry, Academy of Sciences of the Czech Republic, Dolejškova 3, CZ-182 23 Prague 8, Czech Republic

<sup>b</sup> Institute of Chemical Technology, Prague, Faculty of Chemical Technology, Technická 1905/5, CZ-160 00 Prague 6, Czech Republic

Available online 20 December 2006

## Abstract

A new quantitative approach to *in situ* experiments is proposed based on consistent combination of modeling of the relevant processes in the catalyst pellet with realization of the multi-spectroscopic experiment under dynamic regimes. Using well defined Co- and Fe-FER samples the approach is illustrated by three case studies showing potential of the approach for detail analysis of the processes over metallo-zeolites, i.e. adsorption of NH<sub>3</sub> on CoNa-FER, and reactions of selective catalytic reduction of NO by NH<sub>3</sub>, and N<sub>2</sub>O decomposition over Fe-FER. Combination of simultaneous *in situ* FTIR and UV-Vis spectroscopies under transient conditions and a single-pellet reactor model of the spectroscopic cell are used for obtaining some quantitative information on the transport, adsorption/desorption phenomena, and surface species transformation over transition metal ion/zeolite system under such conditions.

© 2006 Elsevier B.V. All rights reserved.

**Keywords:** Metallo-zeolites; FTIR/UV-Vis; Adsorption; Modeling; *in-situ*

## 1. Introduction

The onset of novel nano-technology based catalysts and their optimal application to various uses requires detail understanding of the role of multi-hierarchical structure of catalysts, and its implications for the catalyst performance in real processes. Such structure-related roles include: (i) the action of the active site itself; (ii) host-guest interactions between the active site and the structured support; (iii) the impact of the structural patterns of the support and its micro/mesoporosity. Description of such highly structured system demand understanding also the ways of perturbation of the whole system upon interaction with the reaction media and, moreover, the complex dynamism of the various structural levels at the moment of the catalytic action. For such aim the experiments under transient conditions are usually a method of choice.

For optimal tailoring of metallo-zeolites as hierarchic structures, including cooperation between redox and acidic sites of different natures, as well as the role of transport parameters, obviously necessitates new experimental and

theoretical approaches. Such new approach remains challenging as there are only few true *in situ* or Operando techniques (see e.g. [1]) which could provide relevant structural data, both for the catalyst surface and for the reactive surface species. Moreover, until now most of the *in situ* type studies are limited to providing a qualitative support for a tentative structure-performance concept, and only very rarely produce quantitative data. There are technical reasons for such frequent drawback of the *in situ* or Operando studies: Due to specific demands of the individual spectroscopic techniques the *in situ* spectroscopic measurements are frequently realized under conditions far from optimal arrangement for a standard kinetic study. Obviously, there is a great potential for use of *in situ* type experiments under transient conditions, and at the same time, with experimental arrangement for a direct kinetic analysis of the spectroscopic results.

The concept of transient techniques in heterogeneous catalysis consists of introducing perturbations of one or more experimental variables, such as the gas concentration, reaction temperature or pressure, and the mathematic analysis of the response curve [2–5]. The dynamic response of the system allows determination of the time constants of the surface processes and could be used to obtain both qualitative and quantitative information about the elements of the catalytic reaction.

\* Corresponding author. Tel.: +420 266053646; fax: +420 286582307.

E-mail address: [zdenek.sobalik@jh-inst.cas.cz](mailto:zdenek.sobalik@jh-inst.cas.cz) (Z. Sobalík).

### Nomenclature

$a_v$	relative external surface of microporous crystals ( $m^{-1}$ )
$c_i$	molar concentration of $i$ -th compound in intracrystalline (microporous) domain ( $mol/m^3$ )
$C_i$	molar concentration of $i$ -th compound in intercrystalline (macroporous) domain ( $mol/m^3$ )
$D_{i,p}$	diffusion coefficient of $i$ -th gaseous compound in intercrystalline (macroporous) domain ( $m^2/s$ )
$\bar{D}_i$	diffusion coefficient of $i$ -th gaseous compound intracrystalline (microporous) domain ( $m^2/s$ )
$J_i$	diffusional flux density of $i$ -th compound ( $mol/m^2/s$ )
$k_{C,i}$	external mass transfer mass transfer coefficient ( $m/s$ )
$q_i$	concentration of $i$ -th adsorbed compound ( $mol/m^3$ )
$r$	spatial coordinate of zeolite crystal (m)
$x$	spatial coordinate of pellet (m)

### Greek letters

$\delta$	thickness of catalytic slab (m)
$\delta_c$	characteristic dimension of zeolite crystal (m)
$\varepsilon_p$	catalytic pellet porosity
$\theta_i$	occupancy of $i$ -th compound in (adsorbed) state

### Indexes

o	initial state
$i$	$i$ -th compound
g	gas phase
s	solid state

The present level of time-resolution capability of FTIR and UV-Vis spectroscopy and structural understanding of metallo-zeolites, together with the ability of both spectroscopies to work under true reaction conditions, makes it possible to obtain combined structural and catalytically relevant data. Nevertheless, to preserve the optimal transmission arrangement for infrared quantitative measurements, and at the same time provide for kinetic model construction, the usual flow patterns of the spectroscopic cell must be reversed (see later).

Accordingly, a new approach to the *in situ* experiments, providing for integral use of the chemical-engineering modeling of the dynamic processes in the hierarchic structure of a catalyst, and using a standard pressed pellet, is disclosed and its use is illustrated in several examples.

## 2. Outline of realization

The approach proposed is based on realization of a quantitative version of the *in situ* experiment, i.e. under dynamic conditions and directly providing spectroscopic data for quantitative modeling of the system response. The mathematical description of the experiment has the ambition

to include into the parameters of the model both the individual transport as well as reaction parameters of the catalytic system.

The strategy of the approach could be described in a sequence of two steps: (i) Formulation of a tentative kinetic model of the surface transformations based on previous standard kinetic experiments; (ii) Accumulation of experimental data for solution of the proposed model and optimization of the fit of the experimental data.

The second step provides the best evaluation of the model parameters as well as their statistical relevance. It could also predict conditions for optimal experiments for better parameters estimation. The results would also provide idea for reformulation of the original kinetic model.

The validity of the model evaluation depends strongly on the amount of the relevant experimental data. Accordingly, such high volume of data could be better obtained using complex and dynamic experimental conditions, and eventually, using multi spectroscopic arrangement of the experimental setup.

### 2.1. Experimental

The realized experimental set up should thus provide for quantitative spectroscopic data under conditions, which might be rigorously described by a kinetic model. In combination with the potential of the model used (see later) we aimed into high control of the gas phase composition on the external surface of pellet, while the changes of the composition of the adsorbed species were taken as a response controlled exclusively by the transport and reaction processes inside the material of the pellet.

To obtain a parallel FTIR and UV-Vis spectroscopy results a commercial cell provided by ISRI was modified and a the spectra of the pellet measured by FTIR (Nexus 670, ThermoNicolet) and UV-Vis Avantes Fiber Optic Spectrometer (AvaSpec-2048-TEC-FT-2) under the rapid-scan mode. Under the arrangement used the pellet was measured at the transmission position by FTIR, while at UV-Vis region were taken at the diffusion regime. The scheme of the experimental setup is illustrated at Fig. 1.

The relatively high-volume cell gave only a relatively slow response of the gas outlet composition to a stepwise change of the concentration of the feed. Accordingly, the cell had to be modified by doubling the number of gas in-lets, and by exposing both sides of the pellet directly to the incoming streams, while a broad tube was used for the gas out-let. For

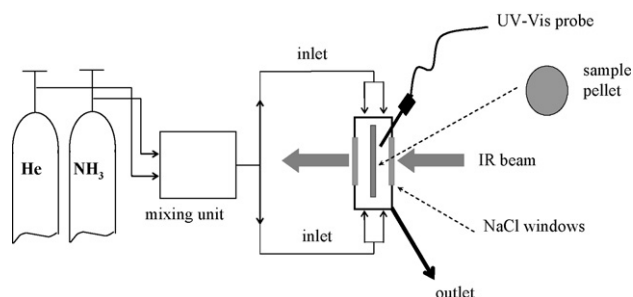


Fig. 1. Scheme of the experimental setup.

such modified cell the CFD modeling of the flow patterns inside the cell, evidenced for high flow rates (over 100 ml/min) a very short response time (<1 s) of the gas phase composition in the vicinity of the pellet walls.

## 2.2. Mathematical model

The spectroscopic cell has been described as a single-pellet reactor with the aim to model the concentration gradients inside the pellet when exposed to various feed compositions changes. Detailed hydrodynamic study using CFD technique reveals that the flow pattern can be represented as a combination of perfectly mixed and plug flow. Due to the experimental arrangement it could be assumed that the composition of the gas phase on the external surface of the pellet is for the model purpose controlled exclusively by the changes in the inlet gas composition, e.g. the real rectangular pulse between  $t = 0$  and  $t = t_{\text{END}}$  has been described by Eq. (1).

$$\begin{aligned} \frac{C_i^o(t)}{\bar{C}_i^o} &= 0 \quad t < \tau_{\text{PFR}}, \quad \frac{C_i^o(t)}{\bar{C}_i^o} \\ &= 1 - \exp\left[-\frac{t - \tau_{\text{PFR}}}{\tau_{\text{CSTR}}}\right] \quad \tau_{\text{PFR}} \leq t \leq t_{\text{END}}, \quad \frac{C_i^o(t)}{\bar{C}_i^o} \\ &= \exp\left[-\frac{t - t_{\text{END}}}{\tau_{\text{CSTR}}}\right] \quad t \geq t_{\text{END}} \end{aligned} \quad (1)$$

The symbols  $\tau_{\text{PFR}}$ ,  $\tau_{\text{CSTR}}$  stand for residence time of plug flow and ideally mixed dead volumes, respectively. The values of  $\tau_{\text{PFR}}$ ,  $\tau_{\text{CSTR}}$  were estimated from CFD calculations and we obtain  $\tau_{\text{PFR}} = 1.19$  s,  $\tau_{\text{CSTR}} = 3.79$  s.

The pellet of the thickness of about 100  $\mu\text{m}$  was taken as a thin slab of bi-porous material, consisting of zeolite crystals with a linear dimension of about 0.1–3  $\mu\text{m}$ . Mass transfer and surface catalytic reactions in such pressed pellet of the porous solids are coupled in complex ways during unsteady-state, dynamic, operation of porous adsorbents and catalysts.

A detailed model of intra particle mass transfer and reaction was developed and used to simulate the response of system. Four mass transfer processes occurring either in parallel or in series can be considered in the analysis [17,18].

- (i) external mass transfer between the gas phase and the external surface of pellet,
- (ii) mass transfer through the intercrystalline voids,
- (iii) adsorption and reaction on the external surface of the zeolite crystals,
- (iv) diffusion, adsorption and reaction in the microporous crystals.

The mass balance equations, boundary and initial conditions describing the species concentration distribution within the pellet having a bimodal texture (intercrystalline space and microporous crystals) are given below. Mass balance in the

intercrystalline voids gives:

$$\varepsilon_{\text{P}} \frac{\partial C_i}{\partial t} = \varepsilon_{\text{P}} D_{i,\text{P}} \frac{\partial^2 C_i}{\partial x^2} + a_{\text{V}} J_i \quad (2)$$

where  $\varepsilon_{\text{P}}$  stands for pellet intercrystalline porosity,  $a_{\text{V}}$  means the external surface of zeolite crystals per unit volume of the pellet,  $D_{i,\text{P}}$  is the effective diffusion coefficient in the intercrystalline voids,  $J_i$  is the diffusional flux on the crystal interface, i.e.

$$J_i = -D_i \left( \frac{\partial c_i}{\partial r} \right)_{r=\frac{\delta}{2}} \quad (3)$$

Boundary conditions and initial conditions are given by symmetry of concentration profile  $C_i(x, t)$  with respect to  $x$  at  $x = 0$  and by equality of fluxes at the external surface of the pellet ( $x = \delta/2$ )

$$\begin{aligned} x = 0, \quad \frac{\partial C_i}{\partial x} &= 0, \quad x = \frac{\delta}{2}, \quad -\varepsilon_{\text{P}} D_{i,\text{P}} \frac{\partial C_i}{\partial x} \\ &= k_{\text{C},i} (C_i - C_i^o(t)) \end{aligned} \quad (4)$$

$$t = 0, \quad C_i(0, t) = 0 \quad (5)$$

Mass balance equations for microporous crystals are given by:

$$\frac{\partial c_i}{\partial t} = \frac{\partial}{\partial r} \left( D_i \frac{\partial c_i}{\partial r} \right) + \sum_{k=1}^{\text{NR}} \nu_{ki} R_k(\mathbf{c}, \boldsymbol{\theta}) \quad (6)$$

$$q_j^{\text{sat}} \frac{\partial \theta_j}{\partial t} = \sum_{k=1}^{\text{NR}} \nu_{kj} R_k(\mathbf{c}, \boldsymbol{\theta}), \quad \theta_j = \frac{q_j}{q_j^{\text{sat}}} \quad (7)$$

where  $D_i(\mathbf{c}, \boldsymbol{\theta})$  is the effective diffusion coefficient involving surface diffusion and gas translational diffusion in microporous space [19],  $c_i$  is the concentration of mobile form of the  $i$ -th species,  $\theta_i$  stands for surface occupancy of  $i$ -th species in micropore and  $q_j$  is the concentration of the  $j$ -th adsorbed species.  $R_k(\mathbf{c}, \boldsymbol{\theta})$  is the reaction rate of the  $k$ -th reaction ( $\text{mol}/\text{m}^3/\text{s}$ ) and  $\nu_{ki}$  represents the stoichiometric coefficient of the  $i$ -th species in the  $k$ -th reaction.

We admit that the mass transfer resistance due to the adsorption on external surface of crystals is negligible. In this case the boundary and initial conditions are:

$$r = 0, \quad \frac{\partial c_i}{\partial r} = 0, \quad r = \frac{\delta_{\text{c}}}{2}, \quad c_i = C_i \quad (8)$$

$$t = 0, \quad c_i(0, r) = 0 \quad (9)$$

Depending on the magnitude of the diffusional and reaction dynamic parameters as well as their relative magnitude, we obtain simplified models which can be used in the data analysis as demonstrated in the next paragraphs.

Transport within the intercrystalline space of the zeolite wafer is assumed to occur by molecular and Knudsen diffusion. Transport within the zeolite crystals is governed by gradient of chemical potential of adsorbed species and the description was based on the Maxwell-Stefan formalism [6].

Mean concentration of  $i$ -th species in the catalyst pellet (i.e. the measurable variable) can be calculated by integration of the concentration profile, i.e.

$$\bar{\theta}(t)_i = \frac{4}{\delta} \int_0^{\delta/2} \int_0^{\delta_c/2} \theta_i(t, x, r) dr dx \quad (10)$$

For construction of the model no assumptions were made about the rate-limiting step, and individual adsorption and reaction steps are described by appropriate reaction schemes. On the other hand, we make the following assumptions in the model: (i) the system is isothermal; (ii) the diffusion coefficients are time and position invariant, the diffusion processes are Fickian; (iii) the adsorption at the micropores follows the Langmuir kinetics.

### 2.3. Methods for solution of the model

The mathematical model expressed by a system of parabolic non-linear partial differential equations was solved numerically by a finite element method using the Lagrange polynomial approximations of arbitrary degree in each of the finite elements, which the interior nodes were optimized as in the orthogonal collocation method (OCMFE) [7–9]. The basic idea of the OCMFE technique, as its name applies, is based on introduction of fixed elements or breakpoints  $\{x_i\}_{i=1}^{NE+1}$  within the integration interval  $(x_1, x_{NE+1})$ , thus forming subdomains. In the development of algorithm based on the method of lines technique, a particular grid of breakpoints has been considered. If the steep gradients of concentration occur we have used Petrov-Galerkin method on moving elements [20]. The resulting system of differential-algebraic equations was solved by the FORTRAN routine DDASPK [10]. The unknown parameters estimation has been done by multi-response nonlinear regression based on the Stewart method using GREG software [11].

### 3. Case studies

To illustrate the potential of this approach for analysis of the adsorption and catalytic performance, results of three different case studies are summarized.

The case studies were realized on metallo-zeolites providing a unique combination of a high level of sample definition, approaching that of a model catalyst, and at the same time present material with a real catalytic significance. Transition metal ions bonded to specific local zeolite framework structures, forming defined cationic sites, exhibit well-defined and unique co-ordinations, and could serve as adsorption or reaction centers [12,13]. For the purpose of the presented case studies, well characterized Co- and Fe-FER samples with low Co/Al ratio were used.

The three cases analyzed differed in the level of complexity as well as the volume of spectroscopic data produced for the model analysis. They included: (i) process of ammonia adsorption on Co/Na-FER, i.e. a system without catalytic reaction and with a high amount of spectroscopic data; (ii)

selective catalytic reduction of  $\text{NO}_x$  by  $\text{NH}_3$  over Fe-FER, i.e. a system with catalytic reaction and high density of spectroscopic data, and (iii) NO accelerated  $\text{N}_2\text{O}$  decomposition over Fe-FER, i.e. a system with catalytic reaction but low extent of spectroscopic experimental data.

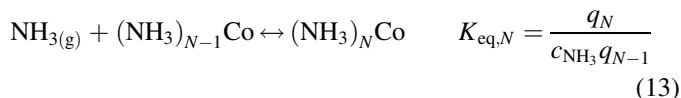
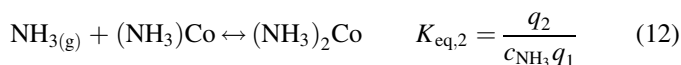
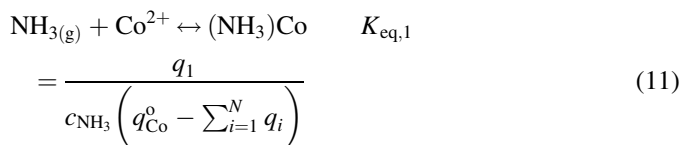
Co/Na-FER, Fe- and Fe/Pt-FER, with M/Al ratio up to 0.2, were prepared using parent zeolite with Si/Al 8.5 (TOSOH) by a method providing for predominant occupation of divalent cation in the established cationic sites. For details on preparation of Co- and Fe-samples as well as identification of the cation positions see e.g. [13] and [14], respectively. Pressed pellets were prepared by a conventional method producing pellet thickness of about 100  $\mu\text{m}$  (approx. the equivalent of about 10  $\text{mg}/\text{cm}^2$ ).

Experimental arrangement for the *in situ* experiments as well as the model solution were used as described above. The measurements were carried at temperatures between 200 and 450  $^\circ\text{C}$  using the modified high temperature catalytic micro-reactor and the gases were fed into the reactor using a PC-controlled mass flow controlled mixing system. The outlet of the cell was connected to a micro-volume GC/IR Interface (Thermo Nicolet) for a gas composition analysis. Details on the gas composition during the individual experiments, and used concentration programs are included in the following paragraphs.

#### 3.1. Formation of extraframework Co- $\text{NH}_3$ complexes in Co/Na-FER

Before experiments the pellet of Co/Na-FER (Co/Al 0.09) was pretreated at the stream of He at 420  $^\circ\text{C}$  for 2 h. The ammonia pulse (1 vol.%  $\text{NH}_3$  in He; length of 10 min) was introduced after stabilization of the system at the He stream under total flow of 100 ml/min at temperature range of 200–400  $^\circ\text{C}$ . During the experiment the time-resolved FTIR and UV-Vis spectra were collected.

Considering a step-wise formation of  $\text{Co}(\text{NH}_3)_n$  complexes during interaction of ammonia with the cobalt cation in a zeolite with Co/Na-FER containing only one type of Co cation site occupation the interaction could be presented as follows:



The system is described by simplified mathematical model based on Eqs. (1)–(10) in which we suppose that only the diffusion in zeolite crystals govern the mass transfer process. Diffusion rate in intercrystalline space is high enough but inside the microporous crystals the diffusion becomes slower, i.e. we

suppose that:

$$\frac{\delta_c^2}{D_i} \gg \frac{\delta^2}{D_{i,p}} \quad (14)$$

where  $\delta_c$  and  $\delta$  are crystal and pellet characteristic dimensions, respectively.

The equilibrium between mobile and adsorbed ammonia in microporous space is assumed. The mass balance equation for ammonia in microporous structure and ammonia adsorbed on cobalt cations becomes:

$$\begin{aligned} \frac{\partial}{\partial t} [\varepsilon_e c_{\text{NH}_3} + (1 - \varepsilon_e) \rho (q_1 + 2q_2)] \\ = \left[ \varepsilon_e + (1 - \varepsilon_e) \rho \left( \frac{\partial q_1}{\partial c_{\text{NH}_3}} + 2 \frac{\partial q_2}{\partial c_{\text{NH}_3}} \right) \right] \frac{\partial c_{\text{NH}_3}}{\partial t} \\ = D_{\text{NH}_3} \frac{\partial^2 c_{\text{NH}_3}}{\partial x^2} \end{aligned} \quad (15)$$

$$q_1 = \frac{q_{\text{Co}}^0 K_{\text{eq},1} c_{\text{NH}_3}}{1 + K_{\text{eq},1} c_{\text{NH}_3} + K_{\text{eq},1} K_{\text{eq},2} c_{\text{NH}_3}^2} \quad (16)$$

$$q_2 = \frac{q_{\text{Co}}^0 K_{\text{eq},1} K_{\text{eq},2} c_{\text{NH}_3}^2}{1 + K_{\text{eq},1} c_{\text{NH}_3} + K_{\text{eq},1} K_{\text{eq},2} c_{\text{NH}_3}^2} \quad (17)$$

The primary FTIR spectroscopic data for simultaneous FTIR and UV-Vis measurement of the CoNa-FER sample response to  $\text{NH}_3$  pulse are illustrated in Fig. 2. The increase of the intensity of the IR band in the NH stretching region between 3520 and 3000  $\text{cm}^{-1}$  was quantified using the steady state data showing distribution between a “bare” Co cation and the  $\text{Co}(\text{NH}_3)_n$  complex [15], and the balance with the total amount of ammonia adsorbed obtained by quantitative evaluation of the FTIR data under all adsorption conditions. We did not assume a change of the extinction coefficient of the NH band at the temperature region analyzed.

This set of nonlinear parabolic partial differential equation was solved by Petrov–Galerkin moving finite elements method. The unknown parameters ( $\delta^2/4D_{\text{NH}_3}$ ,  $K_{\text{eq},1}$ ,  $K_{\text{eq},2}$ ) have been estimated by non linear regression using FORTRAN subroutine GREG [11].

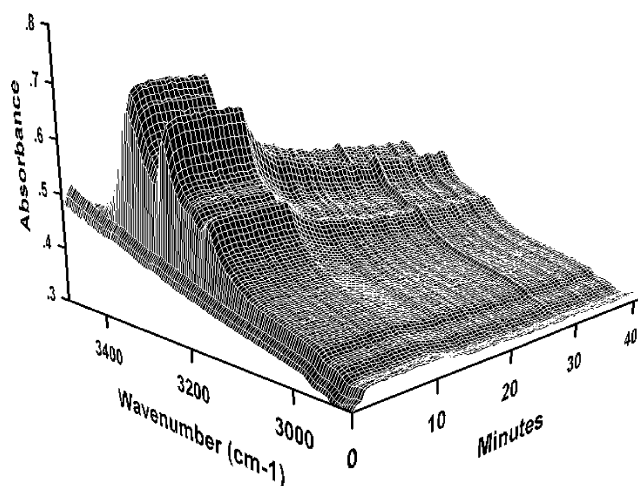


Fig. 2. 3D presentation of the FTIR results of  $\text{NH}_3$  chemisorption on Co/Na-FER.

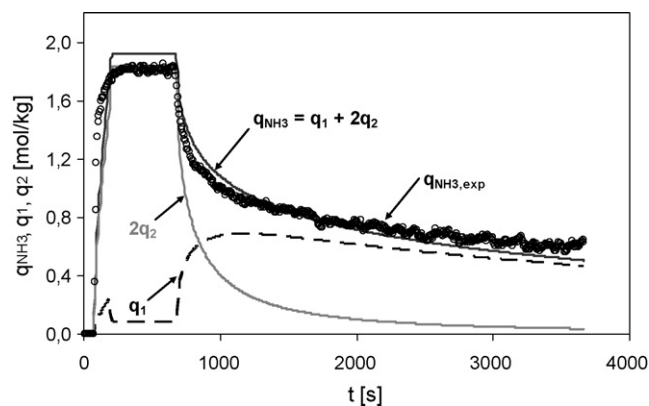


Fig. 3. Analysis of the FTIR results of  $\text{NH}_3$  chemisorption on Co/Na-FER.

The best fit of the experimental data on the ammonia concentration changes produced by the model optimization and the interpretation of the sequence of the individual  $\text{Co}(\text{NH}_3)_n$  complexes formation is illustrated in Fig. 3, showing mean concentrations of total adsorbed ammonia,  $(\text{NH}_3)\text{Co}$  and  $(\text{NH}_3)_2\text{Co}$  defined by:

$$q_{\text{NH}_3}(t) = \frac{2}{\delta} \int_0^{\delta/2} [q_1(x, t) + 2q_2(x, t)] dx \quad (18)$$

and,

$$\bar{q}_1(t) = \frac{2}{\delta} \int_0^{\delta/2} q_1(x, t) dx \quad (19)$$

as a function of time together with experimental values of concentration of total adsorbed ammonia concentration measured by FTIR at 200 °C. The parameters obtained for the optimized model are summarized in Table 1.

The results obtained could be interpreted by formation of ammonia wave propagating into the zeolite crystals and producing a complex with higher amount of  $\text{NH}_3$  ligand, i.e.  $\text{Co}(\text{NH}_3)_{n \geq 2}$ . On the other hand, during desorption the step-wise decomposition of the complex with well established formation of the  $n = 1$  complex is dominant. Simultaneous UV-Vis experiments further support this interpretation, showing a different sequence of UV-Vis spectra during the adsorption and desorption processes.

### 3.2. Selective catalytic reduction of $\text{NO}_x$ by $\text{NH}_3$ over Fe-FER

The data for dynamic analysis of selective catalytic reaction of NO by  $\text{NH}_3$  over Fe-FER sample were provided under the

Table 1  
Adsorption parameters for  $\text{NH}_3$  on Co/Na-FER obtained for the best fit of the model

	200 °C	250 °C	300 °C	350 °C	400 °C
$\delta^2/4D_{\text{NH}_3}$ [1/s]	0.0823	0.0340	0.0579	0.2161	0.1975
$K_{\text{eq},1}$	$2.682 \cdot 10^3$	$2.202 \cdot 10^3$	302.63	14.67	5.059
$K_{\text{eq},2}$	32.59	2.188	$6.87 \cdot 10^{-6}$	–	–



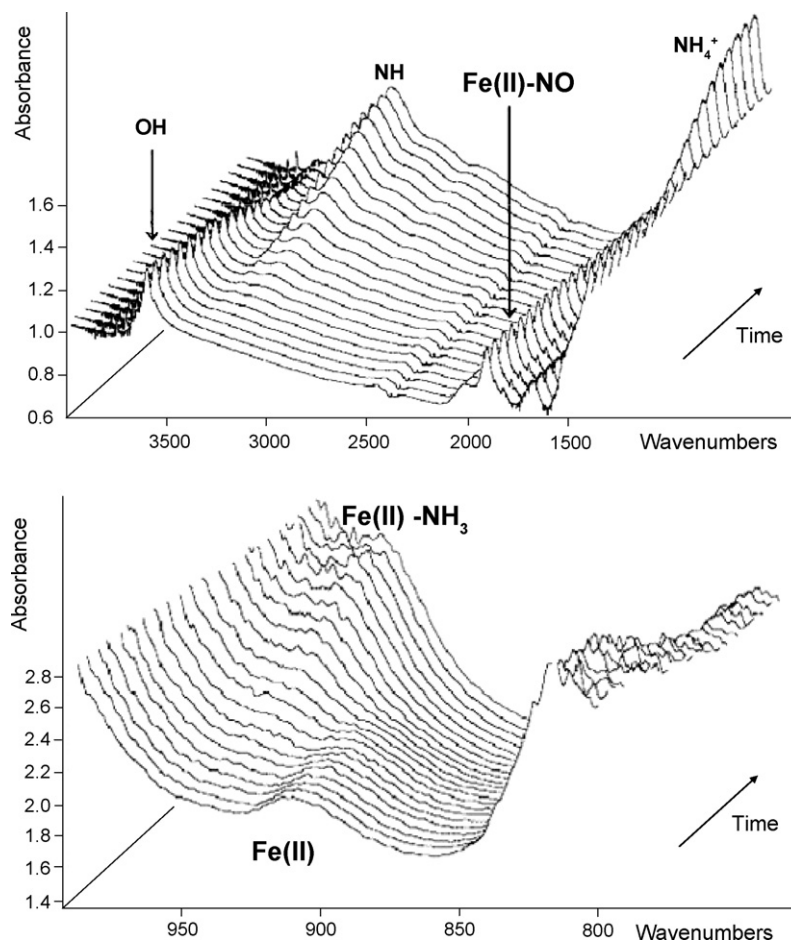


Fig. 4. 3D presentation of the FTIR results during the NO-NH<sub>3</sub> reaction over Fe-FER under the concentration programmed regime.

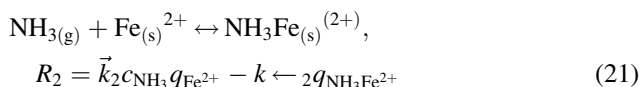
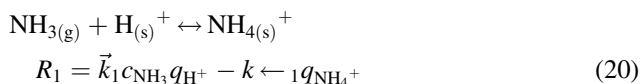
conditions of the Concentration programmed reaction (CPR-FTIR) method (for details see [16]).

Before experiments the pellet of Fe-FER (Fe/Al 0.09) was pretreated at the stream of He with 3% of O<sub>2</sub> at 420 °C for 2 h. Then NO and NH<sub>3</sub> were introduced and their concentrations were repeatedly varied linearly but in the opposite way for the two reacting components and the time-resolved FTIR spectra were collected.

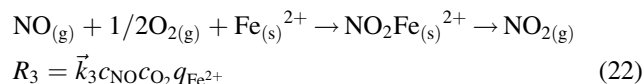
The total flow of the gas mixture in He was 100 ml/min. The experiments under the concentration programmed regime have been realised at temperatures between 200 and 420 °C.

The proposed scheme of the reaction is summarized as follows:

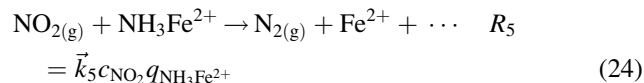
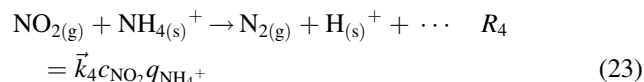
- (1) Ammonia chemisorption on Brönsted sites and Fe<sup>2+</sup> are considered as reversible second order reactions.



- (2) It is assumed that the oxidation of gas phase NO to NO<sub>2</sub> takes place on free Fe<sup>2+</sup> sites. For the purpose of the model we suppose that this reaction is fast and irreversible and the rate is determined by the availability of Fe<sup>2+</sup> sites and concentration of NO and O<sub>2</sub> in micropores.



- (3) Reduction of NO<sub>2</sub> leading to nitrogen takes place both on ammonia adsorbed on Brönsted sites and on Fe<sup>2+</sup> sites.



The 3D presentation of the FTIR results during the NO-NH<sub>3</sub> reaction over Fe-FER sample under the concentration programmed regime is shown at Fig. 4.

The parameters of the model were analyzed based on the experimental data for NH<sub>4</sub><sup>+</sup> and Fe-NH<sub>3</sub>, obtained directly from the FTIR experiments, and includes NH<sub>3</sub>, NO, NH<sub>4</sub><sup>+</sup> and

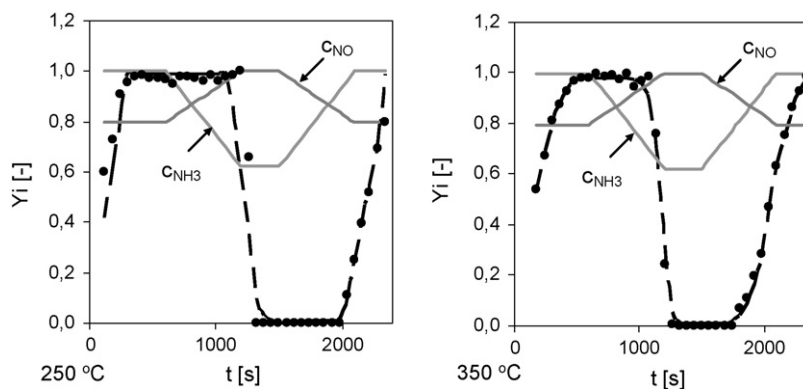


Fig. 5. Experimental and model-predicted data of surface concentrations of  $\text{NH}_4^+$  during the  $\text{NO-NH}_3$  reaction over Fe-FER under the concentration programmed regime at 250 and 350 °C.

Fe– $\text{NH}_3$  mass balance. Mass balances of  $\text{NH}_3$ ,  $\text{NO}$ ,  $\text{O}_2$ ,  $\text{NO}_2$ ,  $\text{NH}_4^+$  and  $\text{NH}_3$  Fe-complex were solved by OCMFE software. As shown at Fig. 5 a close correspondence between experimental and calculated  $\bar{q}_{\text{NH}_4^+}(t)$  profiles was found using following set of kinetic parameters:

$$\vec{k}_1 = 10^3, \quad k_{\leftarrow 1} = \vec{k}_2 = \vec{k}_3 = \vec{k}_5 = 1, \quad \vec{k}_4 = 500. \quad (25)$$

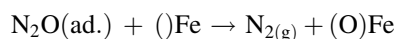
Based on the analysis of the system the well-expressed hysteresis in changes of the concentration of  $\text{NH}_4^+$  induced by opposite changes in the ammonia concentration in the gas phase has been assigned to formation of Fe– $\text{NH}_3$  complexes and effective inhibition of the catalytic role of the bare Fe cations in NO oxidation (for details see [16]).

### 3.3. NO accelerated $\text{N}_2\text{O}$ decomposition

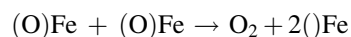
Before experiments the pellet of Fe-FER (Fe/Al 0.12) was pretreated at the stream of He at 420 °C for 2 h. The system was then stabilised in the He stream (100 ml/min) at the

temperatures at the range of 200–400 °C and then a sequence of  $\text{N}_2\text{O}$  and NO pulses were introduced. After stabilization of the system at the He stream under total flow of 100 ml/min the  $\text{N}_2\text{O}$  pulse (length of 15 min, concentration of 1000 ppm of  $\text{N}_2\text{O}$ ) and after 5 min a shorter NO pulse (length of 5 min, concentration of 1000 ppm of NO) were introduced and the time-resolved FTIR spectra collected.

The simplified scheme of the reactions providing for  $\text{N}_2\text{O}$  decomposition and the NO action is summarized as follows. The first step consists of primary decomposition of  $\text{N}_2\text{O}$  on Fe site yielding surface oxygen and gaseous nitrogen:



While the direct recombination of two oxygen atoms, i.e. reaction:



is assumed to be very slow, but it could be accelerated by formation of a secondary NO catalytic site, formed either by adsorption of NO added to the gas phase (NO-accelerated  $\text{N}_2\text{O}$

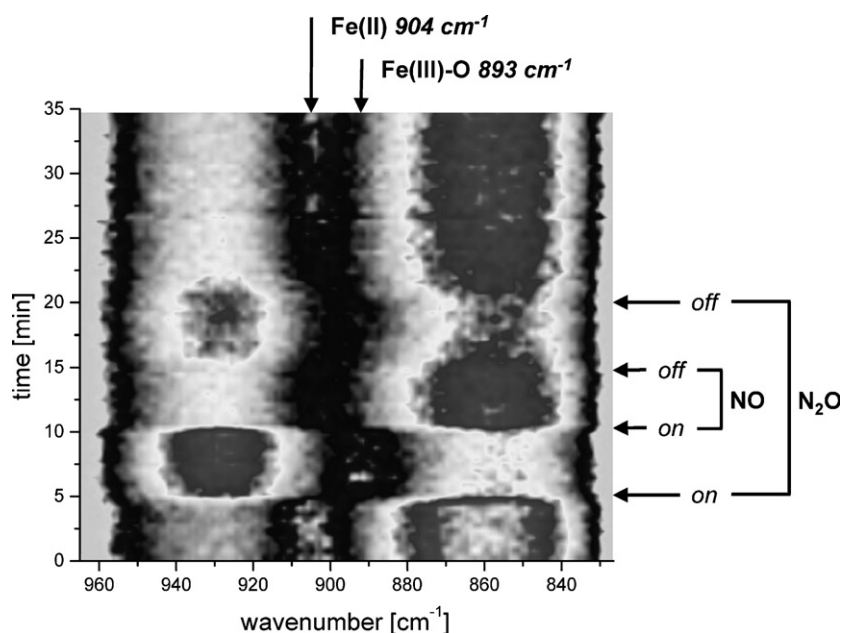
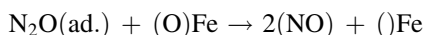


Fig. 6. 3D presentation (Chemigram) of the FTIR results transmission window region of zeolites during the NO assisted  $\text{N}_2\text{O}$  decomposition over Fe-FER.

decomposition regime) or could be formed in the following step catalytic site.



In this system, the available *in situ* spectroscopic data were limited and included information on the changes of the oxidation state of the iron cations bonded into the extra framework positions. Thus only a simple mathematic model could be formulated based on the above tentative reaction scheme and a mass balances of the gaseous and adsorbed species on the catalytic particle and taking into account also the conversion changes obtained over tubular microreactor exposed to the same sequence of  $\text{N}_2\text{O}$  and NO changes.

The 3D presentation of the FTIR spectra of Fe-FER in the region of the transmission window between 980 and 850  $\text{cm}^{-1}$  during a complex sequence of  $\text{N}_2\text{O}$  and NO pulses is presented in Fig. 6. As indicated from the changes of the bands assigned to local perturbation of the zeolite framework due to coordination of Fe(II) (a band at about 904  $\text{cm}^{-1}$ ) and Fe(III)-O (a band at 893  $\text{cm}^{-1}$ ) cations the changes in the oxidation state of Fe-cation was identified in parallel to complex sequence of  $\text{N}_2\text{O}$  and NO pulses. This evidenced prevailing presence of Fe(II) in the He stream, and reversible formation of Fe(III)-O in presence of  $\text{N}_2\text{O}$ , and iron reduction to Fe(II) after NO addition to the  $\text{N}_2\text{O}$  stream. The result of the mathematic analysis supported the existence of a slow (and probably rate determining) step of formal recombination of two oxygen atoms in absence of NO, while in NO presence it identified the  $\text{N}_2\text{O}$  primary splitting and as the relatively slower step (and a candidate for the rate determining step).

Obviously, in this last case the model calculations are supported with only a limited volume of the experimental data could provide only for tentative analysis of the system. Nevertheless, still could offer some background for realistic interpretation of the experimental data.

#### 4. Conclusions

A new approach to *in situ* experiments based on consistent combination of the chemical-engineering type of modeling and realization of the multi-spectroscopic experiment under dynamic regimes on a pressed pellet of metallo-zeolite has been described. It has been shown that the mathematic analysis of the time sequence of the individual transient processes occurring during the concentration modulation have the potential to provide information on the mechanistic and structural background for description of the overall process behavior. Under the arrangement proposed the rates of conversion of the surface species (detected by FTIR or UV VIS) are followed. Accordingly, we propose that in combination with a standard kinetic study, this approach could provide vital data for a complex system analysis.

Using well defined metallo-zeolite samples it was possible to illustrate potential of such methodic approach for analysis of

the dynamic aspects of formation of the metallo-ligand complexes during adsorption experiments ( $\text{NH}_3$  uptake by CoNa-FER), quantitative analysis of dynamic features of a complex reaction including both acidic and redox sites (selective catalytic reduction of NO by  $\text{NH}_3$  reaction over Fe-FER), and for a tentative support at the effort to identify the rate determining step of the complex reaction (NO assisted  $\text{N}_2\text{O}$  decomposition over Fe-FER).

Moreover, such approach has a potential to bridge the gap between the complex nature of the concentration profiles during the dynamic *in situ* experiments over material with multi-hierarchical porous structure and the averaging nature of the spectroscopic experiment, run under transmission optical arrangement.

#### Acknowledgments

The authors acknowledge the support of the projects # 1ET400400413 of ASCR, #104/06/1254 of GACR, and # 203/05/2309 of GAAS.

#### References

- [1] S.J. Tinnemans, M.H.F. Kox, T.A. Nijhuis, T. Visser, B.M. Weckhuysen, *Phys. Chem. Chem. Phys.* 7 (2005) 211.
- [2] K. Tamaru, *Adv. Catal.* 15 (1964) 65.
- [3] K. Tamaru, in: J.R. Anderson, M. Boudart (Eds.), *Catalysis: Science and Technology*, Springer-Verlag, Berlin, 1983, p. 87.
- [4] C. Mirodatos, *Catal. Today* 9 (1991) 83.
- [5] H. Kobayashi, M. Kobayashi, *Catal. Rev. Sci. Eng.* 10 (1974) 139.
- [6] R. Krishna, R. Bauer, *Sep. Purif. Technol.* 33 (2003) 213.
- [7] B. Finlayson, *Nonlinear Analysis in Chemical Engineering*, McGraw-Hill, New York, 1980.
- [8] M. Tayakout, B. Bernauer, Y. Toure, J. Sanchez, *Simul. Pract. Theory* 2 (1995) 205.
- [9] J. Villadsen, M. Michelsen, *Solution of Differential Equation Models by Polynomial Approximation*, Prentice-Hall, Englewood Cliffs, 1978.
- [10] P.N. Brown, A.C. Hindmarsh, L.R. Petzold, *SIAM J. Sci. Comp.* 15 (1994) 1467.
- [11] M. Caracotsios, *Model Parametric Sensitivity Analysis and Nonlinear Parameter Estimation. Theory and Applications*, Ph. D. Thesis, University of Wisconsin-Madison, 1986.
- [12] L. Drozdová, R. Prins, J. Dědeček, Z. Sobalík, B. Wichterlová, *J. Phys. Chem. B* 106 (2002) 2240.
- [13] B. Wichterlová, Z. Sobalík, J. Dědeček, *Appl. Catal. B, Environ.* 41 (2003) 97.
- [14] Z. Sobalík, Z. Tvarůžková, A. Vondrová, M. Schwarze, *Stud. Surf. Sci. Catal.* 162 (2006) 889.
- [15] Z. Sobalík, Z. Tvarůžková, B. Wichterlová, *J. Phys. Chem. B* 102 (1998) 1077.
- [16] Z. Sobalík, J. Nováková, Z. Tvarůžková, M. Schwarze, D. Kaucký, B. Bernauer, *Stud. Surf. Sci. Catal.*, 158 B (2005) 1231.
- [17] D. Do Duong, *Chem. Eng. Sci.* 45 (1990) 1373.
- [18] R.G. Jordi, D. Do Duong, *Chem. Eng. Sci.* 48 (1993) 1993.
- [19] A.J. Burggraaf, *J. Memb. Sci.* 155 (1999) 45.
- [20] R.M. Fuzeland, J.G. Verwer, P.A. Zegeling, *J. Comp. Phys.* 89 (1990) 349.